J Electroceram (2009) 22:390–394
DOI 10.1007/s10832-008-9425-2

Structural evolution and microwave dielectric properties of $(1-x)BaZn_{1/3}Nb_{2/3}O_3+xBaMg_{1/2}W_{1/2}O_3$ ceramics

J. J. Bian · Y. F. Dong · G. X. Song

Received: 18 April 2007 / Accepted: 17 January 2008 / Published online: 31 January 2008

Abstract Structural evolution and microwave dielectric properties of $(1-x)BaZn_{1/3}Nb_{2/3}O_3+xBaMg_{1/2}W_{1/2}O_3$ ($0\leq x\leq 1$) system have been investigated in this work. All samples exhibit single perovskite phase except for the samples with $x=0$ and $x\geq 0.8$ in which barium niobate and $BaWO_4$ second phase existed, respectively. 1:1 cations ordering existed in the samples with $x\geq 0.1$, and the ordering degree increases with the increase of x. Liquid phase sintering was observed in the sample with $x\geq 0.8$. Dielectric constant decreases almost linearly from 40.8 to 17.4 with increasing x. $Q\times f$ value monotonically increases from 26,162 GHz to 64,705 GHz with increasing x. The τ_f value changes from +30 ppm/°C to −27.8ppm/°C. Near zero τ_f value of −1.4 ppm/°C could be obtained at $x=0.4$ composition.

Keywords Perovskite ceramics · Order–disorder · Microwave dielectric properties

1 Introduction

$A^{2+}\left(B^{2+}_{1/3}B^{5+}_{2/3}\right)O_3$ complex perovskites with 1:2 type B-site cation ordering have received widespread interest in the wireless microwave communications community. Previous researches have demonstrated that the microwave dielectric properties of these ceramics are closely related to the degree of cation ordering on the B-site position, given that all other factors are equal. Recently dielectric resonators of Nb-based compounds with a complex perovskite structure have been extensively studied due to their very high quality factor in microwave frequency and relative low cost compared with Ta-based complex perovskite ceramics [1–4]. Among these materials, $BaZn_{1/3}Nb_{2/3}O_3$ (BZN) has been reported to possess high dielectric constant (ε_r~40) compared with $BaZn_{1/3}Ta_{2/3}O_3$ (BZT) (ε_r~30) [3]. The literature values for the $Q\times f$ of BZN are quite varied [2, 3, 5]. The poor reproducibility of Q values was considered to be related to the difficult control of the B-site ordering degree and formation of impurity phases caused by the evaporation of ZnO during sintering process. The highest reported $Q\times f$ value is 87,000 GHz for a well ordered BZN ceramic [5]. However the temperature coefficient of resonant frequency (τ_f) of BZN is relatively high (τ_f ~30 ppm/°C). The tuning of the τ_f value of BZN to zero has been explored in system with a variety of different chemistries [3, 4, 6, 7].The most widespread way to tune τ_f to zero-value is still to form solid solutions between the components having the τ_f value with opposite sign. For example, partial replacement of Zn by Co in solid solutions of $(1-x)BZN+x\ BaCo_{1/3}Nb_{2/3}O_3$ (BCN) results in a zero τ_f value and a high Q value ($Q\times f$=56,000–97,000 GHz) when $x=0.7$ [3]. However its Q value is very sensitive to processing conditions, which was considered to be related to the difficult control of the B-site ordering degree and valence state of Co [2]. Compared with BZT, for BZN, BCN and BZN–BCN solid solutions, the kinetics of cation ordering are considerably slower. Consequently, a slow cooling process [1], long-term sintering[2, 3] or prolonged low-temperature annealing [8, 9] is required to optimize the $Q\times f$ value. Small amount of substitution of W^{6+} for Nb^{5+} accelerates the kinetics of the B-site cation ordering and consequently improves the Q factor of BZN due to the increasing charge difference on B-site [10]. However the substitution of W^{6+} for Nb^{5+} is charge com-

J. J. Bian (✉) · Y. F. Dong · G. X. Song
Department of Inorganic Materials, Shanghai University,
149 Yanchang Road,
Shanghai 200072, China
e-mail: jjbian@shu.edu.cn

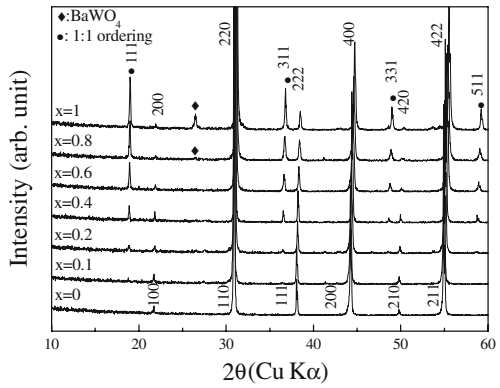

Fig. 1 XRD patterns of $(1-x)$BZN+xBMW ceramics

pensated by the introduction of vacancies on the Zn site, which deviates the B-site composition from 1:2. The presence of high concentration of B-site vacancies usually destabilize a cubic perovskite [10].

$Ba(Mg_{1/2}W_{1/2})O_3$ (BMW) doped with small amount of Ti on B-site was reported to have high quality factor ($Q\times f$~107,000 GHz) and negative τ_f value (~−34ppm/°C) [11]. The average ionic radii of B-site cations in BMW is 0.66 Å, which is slightly smaller than that in BZN (0.673 Å). Therefore, $(1-x)$BZN+xBMW might form solid solutions and are expect to obtain a new material which has the zero τ_f value. The crystal structure of BMW is cubic with 1:1 rock-salt pattern of ordering on B-site due to large charge difference between B-site cations [11]. Therefore the co-substitution of $(Mg_{1/2}W_{1/2})^{4+}$ for $(Zn_{1/3}Nb_{2/3})^{4+}$ is charge and site balanced, and might make the B-site ordering transform from 1:2 to 1:1. The present work is focused on the structural evolution and microwave dielectric properties of BZN–BMW system.

2 Experiment

$(1-x)BaZn_{1/3}Nb_{2/3}O_3+xBaMg_{1/2}W_{1/2}O_3$ $(0\le x\le 1)$ ceramic samples were prepared by conventional solid-state reaction process from the starting materials including Nb_2O_5 (99.9%), CoO(99.8%), $BaCO_3$(99.7%, WO_3(99.6%), MgO(99.5%) and ZnO(99.6%). The raw materials were weighed according to the formula of $(1-x)BaZn_{1/3}Nb_{2/3}O_3+xBaMg_{1/2}W_{1/2}O_3$ $(0\le x\le 1)$ and milled with ZrO_2 balls in ethanol for 24 h. The wet mixed powders were dried and calcined at the temperature of 1200–1250 °C for 2 h in a alumina crucible. The calcined powders were reground for 24 h, dried, mixed with 7 wt.% PVA as binder and granulated. The granulated powders were uni-axially pressed into compacts with 10 mm in diameter and 4–5 mm in height under the pressure of 100 Mpa. The compacts were sintered between 1400–1550 °C for 10 h. The sintering temperature increased with the increase of BMW content. A cooling rate of 100 °C/h was employed. In order to prevent the Zn evaporation loss, the compacts were muffled with powder of the same composition.

The phase constituents of the sintered samples were identified by X-ray powder diffraction (XRD) with Ni-filtered CuKα radiation (40 Kv and 20 mA, Model Dmax-RC, Japan). In order to avoid the influence of the second phases formed on the surface during sintering, the surface of the specimen for XRD was abraded. The unit cell parameter was calculated from the obtained XRD data by Jade 5.0 software. Bulk densities of the sintered specimens were identified by the Archimedes' method. The microstructure of the sintered sample was characterized by scanning electron microscopy (SEM) (Model XL20, Philips Instruments, Netherlands). All samples were polished and thermally etched at a temperature which was 200 °C lower than its sintering temperature. Microwave dielectric properties of the sintered samples were measured between 7 and 8 GHz using network analyzer (Hewlett Packard, Model HP8720C, USA). The quality factor was measured by the transmission cavity method. The relative dielectric constant (ε_r) was measured according to the Hakki–Coleman method using the TE_{011} resonant mode, and the temperature coefficient of the resonator frequency (τ_f) was measured using invar cavity in the temperature range from 20 to 80 °C.

3 Results and discussions

Figure 1 shows the XRD patterns of $(1-x)BaZn_{1/3}Nb_{2/3}O_3+xBaMg_{1/2}W_{1/2}O_3$ $(0\le x\le 1)$ ceramics. Phase analysis of the XRD patterns show that all samples exhibit single perovskite phase except for the samples with $x\ge 0.8$ in which small amount of $BaWO_4$ second phase existed. The content of $BaWO_4$ increases with x. This is consistent with the findings of D.D. Khalyavin et al. for the $LaMg_{1/2}Ti_{1/2}O_3$–$BaMg_{1/2}W_{1/2}O_3$ system [12, 13]. The presence of $BaWO_4$ secondary phase in BMW ceramics was considered to be due to the thermal decomposition of the BMW perovskite phase above the temperature of 1200 °C [13]. Therefore

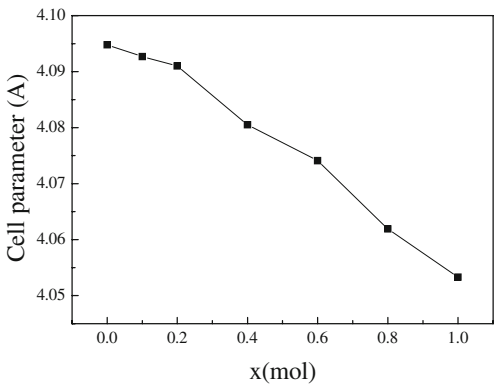

Fig. 2 Variation of unit cell parameter as function of x

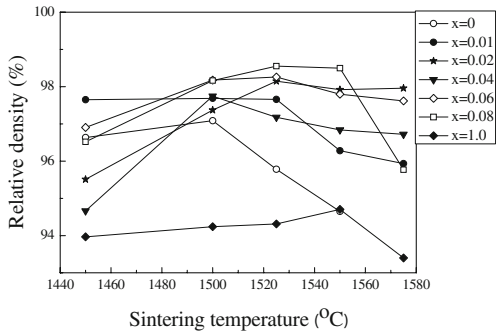

Fig. 3 Variation of relative density for $(1-x)BaZn_{1/3}Nb_{2/3}O_3+xBaMg_{1/2}W_{1/2}O_3$ $(0\le x\le 1)$ as function of sintering temperature

the formation of $BaWO_4$ secondary phase in BMW-riched BZN–BMW solid solutions appears to be caused by the thermal instability of the solid solution due to the increase of BMW content. No superlattice reflections caused by 1:2 long range ordering was observed for the all obtained samples. It may be related to its higher sintering temperature (≥1450 °C). It was reported that 1:2 order–disorder transformation temperature is about 1375 °C [14–16]. Sintering above the transformation temperature and fast cooling rate would result in the structure disordering. As expected, however, superlattice reflections from 1:1 B-site cations ordering could be easily observed for the samples with $x\ge 0.1$ due to the large charge difference between Mg^{2+} and W^{6+}. Its intensity increases with the increase of x, which means the 1:1 ordering degree increases with increasing BMW content. With the addition of BMW, increase of 1:1 ordering is reasonable, as the total B-site cations ratio is approaching to 1:1 rather than 1:2. The variation of unit cell parameter as function of x is shown in Fig. 2. The cell parameter linearly decreases with the increase of x due to the B-site substitution of smaller (Mg^{2+} W^{6+}) (R^{2+}_{Mg}: 0.072 nm, R^{6+}_{W}: 0.058 nm) for (Zn^{2+} Nb^{5+}) (R^{2+}_{Zn}: 0.074 nm, R^{5+}_{Nb}: 0.069 nm) cations, which means that solid solutions are formed in all the range of $(1-x)$BZN+xBMW compositions.

In order to calculate the relative density of the sintered samples, the theoretical density of each composition was estimated from the obtained formula and cell parameters. Accurate theoretical density was not easy to obtain for the samples with $x\ge 0.8$ due to the presence of multiphase. $BaWO_4$ phase was excluded from the calculation of theoretical density for the samples with $x\ge 0.8$. The theoretical density of $BaWO_4$ is 6.39 g/cm^3, which is lower than that of $Ba(Mg_{1/2}W_{1/2})O_3$ (7.22 g/cm^3). Therefore the presence of $BaWO_4$ phase resulted in the lowing estimated relative density of theoretical density (TD). Figure 3 illustrates variation of relative density for $(1-x)BaZn_{1/3}Nb_{2/3}O_3+xBaMg_{1/2}W_{1/2}O_3$ $(0\le x\le 1)$ as function of sintering temperature. All samples could be sintered to >96% TD except for the $x=1.0$ sample. Our confusion is that we could not obtain a densified BZN sample when the sintering temperature was lower than 1400 °C. The sintering temperature is 100°C higher than the reported one. This is may be related to the raw materials we used. Figure 4

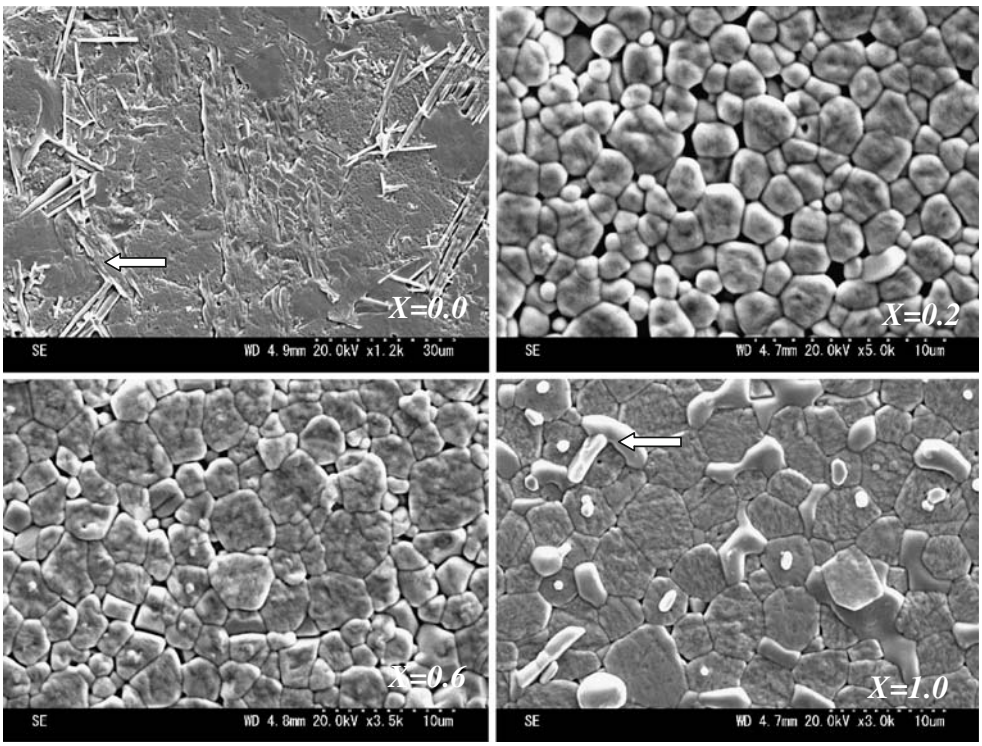

Fig. 4 SEM micrographs of $(1-x)$BZN+xBMW cermics ($x=0$, 0.2 samples sintered at 1500 °C/2 h and $x=0.6$, 1.0 samples sintered at 1550 °C/2 h, respectively)

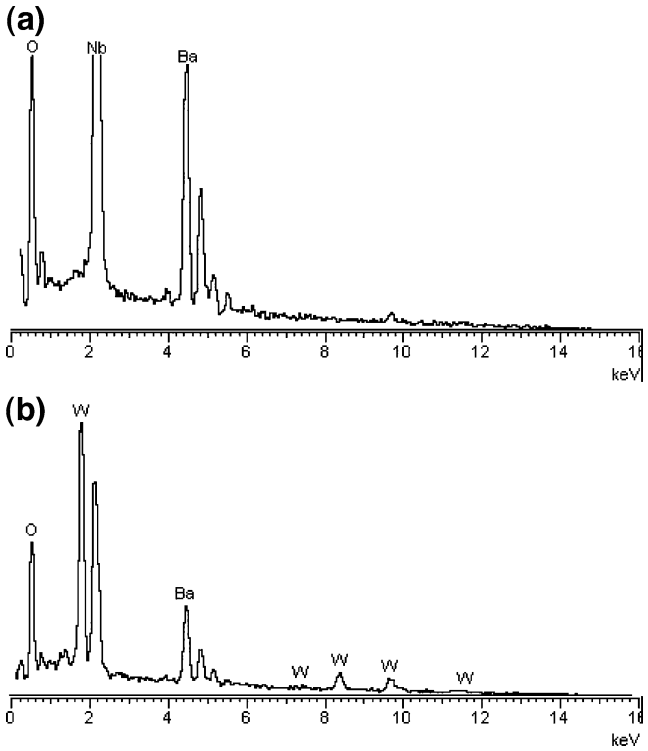

Fig. 5 EDS analysis for (**a**) plate-like second phase marked by arrow in the x=0 sample (**b**) second phase marked by arrow in x=1.0 sample

shows the typical SEM micrographs for the x=0, 0.2 samples sintered at 1500 °C/2 h and x=0.6, 1.0 samples sintered at 1550 °C/2 h, respectively. The x=0.2 and x=0.6 samples exhibit homogeneous microstructure. However plate-like second phase was observed in x=0 sample, which is not agreement with XRD analysis. The composition of the plate like second phase marked by arrow was identified as barium niobate (Ba: 20.61, Nb: 23.17 and O: 56.21 at.%) by energy dispersive X-ray (EDS) analysis [Fig. 5(a)]. The formation of barium niobate second phase is due to the zinc evaporation during sintering process although the compacts were muffled with powder of the same composition. Because the peak positions in XRD patterns for most of the barium niobate compounds such as $BaNbO_{3.06}$ and $Ba_{0.99}NbO_{3.06}$ etc are almost coincide with

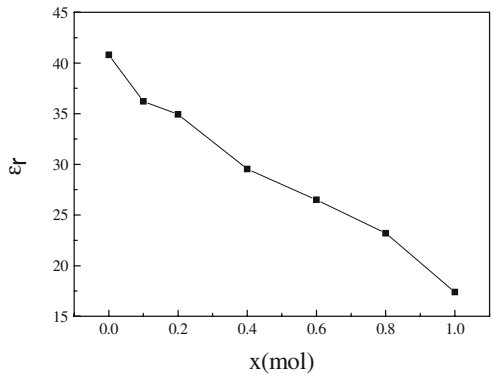

Fig. 6 Variation of dielectric constant as function of x

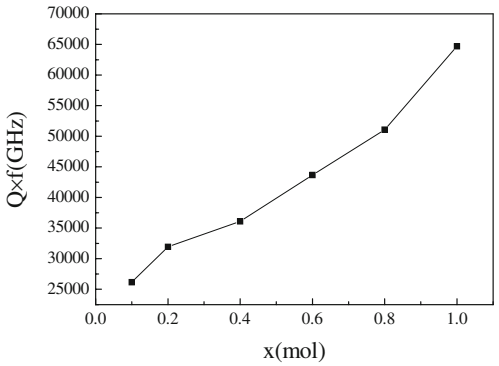

Fig. 7 Variation of Q×f value as function of x

that of BZN. So it is difficult to observe the existence of barium niobate second phase in XRD patterns. The disordering on B-site cations for BZN is related to the presence of barium niobate second phase, which is agreement with the results of K. S. Hong et al. [15] and J. K. Park et al. [17] A unique feature of the microstructure was observed in the sample with x=1.0, where a liquid phase formed in the grain boundary junction of matrix. The composition of the liquid phase was identified as $BaWO_4$ (Ba:16.51, W: 17.84, O:65.65 at.%) by EDS analysis [Fig. 5(b)], which is agreement with the XRD analysis. The melting point of $BaWO_4$ is 1435 °C [18]. In this respect, the $BaWO_4$ liquid phase was expected to appear during sintering at 1550 °C and crystallize during cooling. With the appearance of the liquid phase during sintering, materials transfer was accelerated and consequently notable growth in grain size should occur. The average grain size in x=0.2 sample is about 1–2 μm, whereas, the average grain size in BMW ceramics is about 5–6 μm. The increase in grain size is very limited. As we know, the sinterability improvement of liquid phase sintering is much related to the wetting ability between the liquid phase and matrix grain. From the rounded shape of liquid phase surface regions exposed at the triple junctions, the wetting ability between the liquid phase and matrix grains is poor.

The microwave dielectric properties of ceramics depend on the synthesizing conditions. Hence the calcinations and

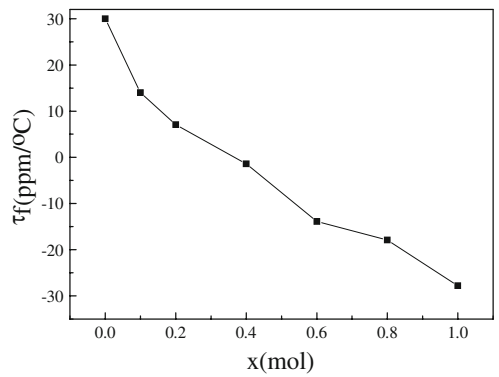

Fig. 8 Varation of τ_f as function of x

sintering temperatures were optimized to get the best densification and microwave dielectric properties. Variation of dielectric constant with x is shown in Fig. 6. The dielectric constant decreases almost linearly from 40.8 to 17.4 with increasing x, which is related to the increasing content of BMW (ε_r~17.6) [13] and $BaWO_4$(ε_r~8) [19–21]. Variation of Q×f value as function of x is shown in Fig. 7. Q×f value monotonically increases from 26,162 GHz to 64,705 GHz with increasing x, which is mainly due to the increase of 1:1 B-site ordering degree. The Q×f value of BZN is much lower compared with the reported value (87,000 GHz) [5], which is related to the disordering on B-site and presence of barium niobate second phase. Many authors reported that BZN with high density and large grains still exhibited relatively high Q factor regardless the structure disordering. But the Q factor should be affected by the type of impurity phases. In our experiment, the composition of impurity phase is different from the reported ones due to higher sintering temperature (1500 °C). Another possible reason may be caused by the contamination of Zr during milling process. We think that if we could obtain pure densified 1:2 ordering BZN its 1:2 ordering would decrease and transform into 1:1 ordering with increasing BMW content. The Q factor of the pure ordering BZN may be much higher than the present one and decreases with the decrease of 1:2 ordering up to some x value and then increase with the further increase of x. Q×f value of $BaWO_4$ was reported to be varied from 16,000 to 57,500 GHz [19–21]. The existence of $BaWO_4$ second phase does not deteriorate the Q×f value of BMW-rich compositions seriously. It indicates that the factor of 1:1 B-site ordering degree influencing the Q×f value dominated over other factors such as second phase and porosity when $x \geq 0.1$. Figure 8 shows the variation of temperature coefficient of resonant frequency τ_f as function of x. The τ_f value monotonically changes from +30 ppm/°C to −27.8 ppm/°C. Near zero τ_f value of −1.4 ppm/°C could be obtained at x=0.4 composition.

4 Conclusions

Structural evolution and microwave dielectric properties of $(1-x)BaZn_{1/3}Nb_{2/3}O_3+xBaMg_{1/2}W_{1/2}O_3$ ($0 \leq x \leq 1$) system have been investigated in this work. Solid solutions are formed in all the range of $(1-x)$BZN+xBMW system. Small amount of $BaWO_4$ second phase exists in the samples with $x \geq 0.8$. Barium niobate second phase was observed in the BZN sintered sample. Superlattice reflections from 1:1 rather than 1:2 B-site cations ordering could be easily observed for the samples with $x \geq 0.1$ due to the large charge difference between Mg^{2+} and W^{6+}. The 1:1 cation ordering degree increases with increasing BMW content. Dielectric constant decreases and Q×f value increases almost linearly with increasing x. The τ_f value monotonically changes from positive to negative value, and near zero τ_f value could be obtained nearby x=0.4 compositions.

Acknowledgement This work was supported by the National Science Foundation of China (NSFC), (project number: 50572060), and by the Shanghai Pujiang Program(D)".

References

1. R.I. Scott, M. Thomas, C. Hampson, J. Eur. Ceram. Soc. **23**, 2467 (2003)
2. K. Endo, K. Fujimoto, K. Murakawa, J. Am. Ceram. Soc. **70**(9), 215 (1987)
3. C.-W. Ahn, H.-J. Jang, S. Nahm, H.-M. Park, H.-J. Lee, J. Eur. Ceram. Soc. **23**, 2473 (2003)
4. H. Hughes, D.M. Iddles, Appl. Phys. Lett. **79**(18), 2952 (2001)
5. S. Nomura, Ferroelectrics, **49**(1–4), 61 (1983)
6. I.M. Reaney, E.L. Colla, N. Setter, Jpn. J. Appl. Phys. **33**, 3984 (1994)
7. S.Y. Cho, H.J. Youn, K.S. Hong, I.T. Kim, Y.H. Kim, J. Mater. Res. **12**(6), 1558 (1997)
8. I.T. Kim, Y.H. Kim, S.J. Chung, J. Mater. Res. **12**(2), 518 (1997)
9. I.T. Kim, Y.H. Kim, S.J. Chung, Jpn. J. Appl. Phys. **34**, 4096 (1995)
10. H. Wu, P.K. Davies, J. Am. Ceram. Soc. **89**(7), 2271 (2006)
11. H. Takahashi, K. Ayusawa, N. Sakamoto, Jpn. J. Appl. Phys. **36**, 5597 (1997)
12. D.D. Khalyavin, A.N. Salak, M.P. Seabra, A.M.R. Senos, P.Q. Mantas, V.M. Ferreira, Mater. Res. Bull. **41**, 167 (2006)
13. D.D. Khalyavin, J. Han, A.M.R. Senos, P.Q. Mantas, J. Mater. Res. **18**, 2600 (2003)
14. M.A. Akbas, P.K. Davies, J. Am. Ceram. Soc. **81**(4), 1061 (1998)
15. K.S. Hong, I.T. Kim, C.D. Kim, J. Am. Ceram. Soc. **79**(12), 3218 (1996)
16. B.K. Kim, H.O. Hamaguchi, I.T. Kim, K.S. Hong, J. Am. Ceram. Soc. **78**(11), 3117 (1995)
17. J.K. Park, D.Y. Kim, Acta Mater. **49**, 631 (2001)
18. L.L.Y. Chang, M.G. Scroger, B. Phillips, J. Am. Ceram. Soc. **49** (7), 385 (1966)
19. S. Nishigaki, S. Yano, H. Kato, J. Am. Ceram. Soc. **71**(11), 385 (1988)
20. S.H. Yoon, D.-W. Kim, S.-Y. Cho, K.S. Hong, J. Eur. Ceram. Soc. **26**, 2051 (2006)
21. K. Yan, Z.F. Gao, J.J. Bian, J. Chin. Ceram. Soc. **l2**, 251 (2006)